



# TECHNICAL NOTE

D-1281

ANALYTICAL AND EXPERIMENTAL INVESTIGATION OF FORCES  
AND FREQUENCIES RESULTING FROM LIQUID  
SLOSHING IN A SPHERICAL TANK

By Andrew J. Stofan and Alfred L. Armstead

Lewis Research Center  
Cleveland, Ohio

NATIONAL AERONAUTICS AND SPACE ADMINISTRATION  
WASHINGTON

July 1962

1. The first part of the document is a list of names and titles.

2. The second part of the document is a list of names and titles.

3. The third part of the document is a list of names and titles.

4. The fourth part of the document is a list of names and titles.

5. The fifth part of the document is a list of names and titles.

6. The sixth part of the document is a list of names and titles.

## NATIONAL AERONAUTICS AND SPACE ADMINISTRATION

TECHNICAL NOTE D-1281

ANALYTICAL AND EXPERIMENTAL INVESTIGATION OF FORCES  
AND FREQUENCIES RESULTING FROM LIQUID  
SLOSHING IN A SPHERICAL TANK

By Andrew J. Stofan and Alfred L. Armstead

## SUMMARY

An analytical and experimental study was conducted to determine the natural frequencies and forces of liquid oscillations in a spherical tank. An integral-equation approach was used to study the oscillations and the natural modes of sloshing in the nearly full to nearly empty tank. The results of the theoretical calculations are in good agreement with the experimentally determined slosh forces except at frequencies very close to the natural modes and are in excellent agreement with the experimental frequencies for various liquid depths.

## INTRODUCTION

For space vehicles containing relatively large masses of liquid propellants, sloshing is a potential source of disturbance critical to the stability of the vehicle. Oscillations may result, for example, from attitude-stabilization-control pulses, and can exert forces and moments on the vehicle that cause a shift in the center of gravity. The most critical situation occurs at a point where the excitation frequency and the fundamental frequency of the contained liquid are nearly the same.

As reported in the literature, the natural frequencies and, to a lesser extent, the forces of liquid sloshing in specific tank configurations of various sizes have been investigated analytically and experimentally (refs. 1 to 9). Because of the potential of minimum weight for a given propellant volume, spherical tanks are strong contenders for space-vehicle applications. Prior to this investigation, information on spherical tanks included: (1) an analytical method for the prediction of the natural frequencies of contained liquids for the special cases of empty, half-full, and full tanks (ref. 10), (2) analytical equations to predict slosh forces (refs. 10 and 11), and (3) experimentally determined natural frequencies for a full range of liquid depths (reported and

compared with frequencies determined analytically by the method of item (2) in ref. 12). Obviously missing are data for experimentally determined slosh forces and an experimentally verified method for predicting forces and natural frequencies at arbitrary liquid depths.

An analytical and experimental investigation of liquid oscillations in a nearly empty to nearly full spherical tank was conducted at the NASA Lewis Research Center. The analytical investigation assumed a non-viscous liquid, and the experimental program used liquids having viscosities of approximately 1 centipoise. Both investigations were conducted for unrestricted liquid sloshing; that is, there were no slosh-suppression devices used. In the analysis the analytical equations of reference 10, relating to the modes and frequencies of specific liquid depths, were augmented and modified; and equations applicable at arbitrary liquid depths were obtained. These modified equations and the force equations of references 10 and 11 were then applied to prediction of the natural frequencies and the slosh forces. Experimental verification of the analysis was provided by measurement of natural frequencies and slosh forces from oscillatory frequencies that extended through the first two natural modes of the contained liquid. The analytical predictions and experimental results are compared herein.

#### SYMBOLS

|                                |   |
|--------------------------------|---|
| A                              | kernel function for spherical tank                        |
| a,e, $\beta$                   | parameters related to tank depth                          |
| C <sub>n</sub> ,D <sub>n</sub> | modal parameters  |
| d                              | diameter, ft  |
| E,K                            | elliptic integrals (of first and second kind)             |
| F <sub>s</sub>                 | slosh force acting on container, lb                       |
| F <sub>t</sub>                 | external transversal force acting on container, lb        |
| G                              | velocity potential  |
| g                              | vertical acceleration of tank, 32.174 ft/sec <sup>2</sup> |
| h                              | liquid depth, ft  |
| i,j,n                          | integers (1,2,3, . . . , N)                               |
| L                              | constant  |

|                                       |  |
|---------------------------------------|--|
| $M_C$                                 | mass of container, slugs                             |
| $M_L$                                 | mass of liquid, slugs                                |
| $N$                                   | order of the matrix                                  |
| $R$                                   | sphere radius, ft                                    |
| $r, Y, \theta$                        | cylindrical coordinate system                        |
| $S_b$                                 | rigid wetted boundary surface, sketch (a)            |
| $S_f$                                 | free surface   |
| $T$                                   | integrating diagonal matrix of order $N$             |
| $t$                                   | time   |
| $u$                                   | transverse displacement of container, ft             |
| $V_X, V_Y, V_Z$                       | velocities in X-, Y-, and Z-directions, respectively |
| $W_n, f(\rho)$                        | wave forms for spherical parameters                  |
| $X, Y, Z$                             | geometric coordinate system, sketch (a)              |
| $X_0$                                 | amplitude of tank displacement, ft                   |
| $\alpha$                              | induced excitation frequency, radians/sec            |
| $\alpha\sqrt{R/g}$                    | oscillatory frequency parameter                      |
| $\Gamma$                              | $\rho/\bar{\rho}$                                    |
| $\gamma$                              | $\frac{\pi}{\frac{\pi}{2} + \beta}$                  |
| $\Delta$                              | interval of subdivision (step size), $1/N$           |
| $\epsilon$                            | $\rho - \bar{\rho}$                                  |
| $\lambda$                             | $\omega_n^2 R/g$                                     |
| $\sqrt{\lambda}$                      | natural frequency parameter, $\omega_n \sqrt{R/g}$   |
| $\rho, \bar{\rho}, \eta, \theta, \xi$ | nondimensional coordinates                           |
| $\rho_L$                              | density of liquid, slugs/cu ft                       |

|            |                                 |
|------------|---------------------------------|
| $\sigma_n$ | slosh height, ft                |
| $\phi$     | velocity potential              |
| $\omega$   | circular frequency, radians/sec |

### EXPERIMENTAL APPARATUS AND PROCEDURE

The experimental apparatus is shown in figures 1 and 2. A 9.5-inch-diameter spherical tank was formed in a lucite block. The block was mounted on ball bearings and was free to oscillate in a horizontal plane. The oscillatory motion of the block was provided by a driving mechanism powered by an electric motor. The driving amplitude could be varied from 0 to 1 inch and the frequency from 0 to 5 cycles per second. The electric motor was wired so that alternating current could be removed from the field and direct current supplied to one of the windings. Then the oscillatory motion could be "quick-stopped," and the horizontal forces resulting from the liquid motion only could be measured. These forces were sensed by a strain gage mounted between the lucite block and the driving mechanism. The signal from the strain gage was recorded by a continuously recording strip chart.

In order to cover a range of densities and forces for a given amplitude, water and mercury were used as test liquids.

The block was oscillated at a preselected frequency, amplitude, and liquid depth and then quick-stopped. The residual horizontal slosh forces and frequencies were recorded. A typical trace of slosh forces is shown in figure 3. For each liquid depth, the frequency was varied from zero through the first two natural modes of the contained liquid. The amplitude of oscillation was selected so that the wave forms were clearly defined at the natural modes.

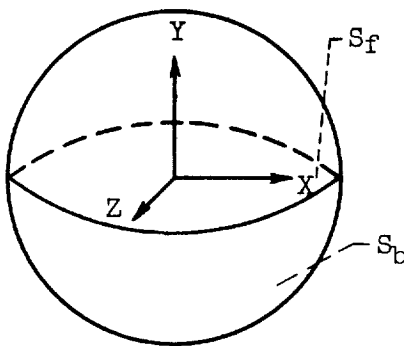
The experimental values of frequency, liquid depth, and slosh forces were reduced to dimensionless parameters by similitude theory (ref. 1). The independent variables, liquid-depth ratio  $h/2R$  and oscillatory frequency parameter  $\alpha\sqrt{R/g}$ , were varied from 0 to 1 and 0 to 3, respectively.

### ANALYSIS AND COMPARISON WITH EXPERIMENT

#### Introduction to Basic Analytical Equations

The motion is that of a liquid bounded by a horizontal free surface  $S_f$ , and a rigid wetted boundary surface  $S_b$ ; small harmonic oscillations

are assumed (sketch (a)). The velocities in the X-, Y-, and Z-directions



(a) Sketch of spherical tank showing free surface  $S_f$ , and wetted boundary surface  $S_b$ .

are defined by the equations (ref. 10)

$$V_X(X,Y,Z)\sin \omega t \quad (1)$$

$$V_Y(X,Y,Z)\sin \omega t \quad (2)$$

$$V_Z(X,Y,Z)\sin \omega t \quad (3)$$

Assuming the motion to be irrotational, a velocity potential  $\phi$  will exist, where

$$V_X = \frac{\partial \phi}{\partial X} \quad (4)$$

$$V_Y = \frac{\partial \phi}{\partial Y} \quad (5)$$

$$V_Z = \frac{\partial \phi}{\partial Z} \quad (6)$$

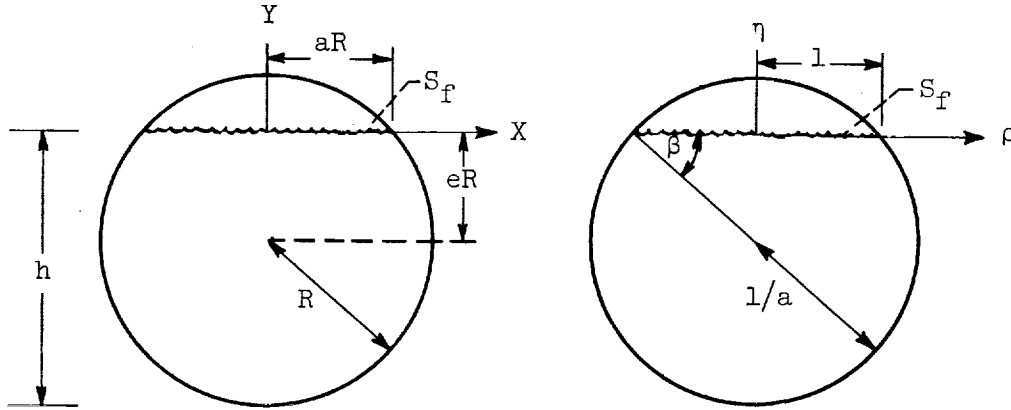
and the continuity equation for incompressible flow will be

$$\nabla^2 \phi = 0 \quad (7)$$

The condition of constant pressure at the free surface  $S_f$ , together with the linearized Bernoulli equation, gives

$$\frac{\partial \phi}{\partial Y} = \frac{\omega^2}{g} \phi \quad (8)$$

on the free surface. Sketches (b) and (c) show the geometrical and non-dimensional parameters, respectively, for the partially filled spherical tank where the depth of liquid is measured by  $e$  varying from  $-1$  for the empty tank to  $1$  for the full tank.



(b) Geometrical parameters for spherical tank.

(c) Nondimensional parameters for spherical tank.

It is convenient to nondimensionalize the system by introducing

$$\rho = \frac{X}{aR} \quad (9)$$

$$\eta = \frac{Y}{aR} \quad (10)$$

Introduction of the cylindrical coordinate system gives

$$X = r \cos \theta \quad (11)$$

$$Z = r \sin \theta \quad (12)$$

For the nondimensional system  $(\rho, \eta, \theta) = (r, Y, \theta)$ ; then

$$\rho = \frac{r}{aR} \quad (13)$$

$$\eta = \frac{Y}{aR} \quad (14)$$

The free-surface condition becomes

$$\frac{\partial \phi}{\partial \eta} = (\lambda a) \phi \quad (15)$$

The angle  $\beta$  is defined as

$$\beta = \sin^{-1}e \quad (16)$$

and varies from  $\pi/2$  for the full tank to  $-\pi/2$  for the empty tank. The governing differential equation for the spherical tank is defined (in nondimensional cylindrical coordinates) as:

$$\frac{\partial^2 \varphi}{\partial \rho^2} + \frac{1}{\rho} \frac{\partial \varphi}{\partial \rho} + \frac{\partial^2 \varphi}{\partial \eta^2} + \frac{1}{\rho^2} \frac{\partial^2 \varphi}{\partial \theta^2} = 0 \quad (17)$$

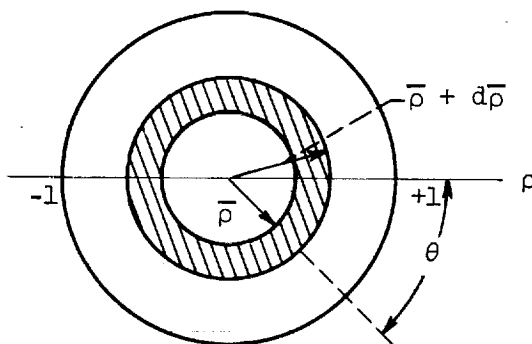
where  $\varphi$  is the velocity potential denoted by

$$\varphi = f(\bar{\rho})G(\rho, \eta, \theta, \bar{\rho})\bar{\rho} d\bar{\rho} \quad (18)$$

The solution then is in the form

$$f(\rho) = \lambda a \int_0^1 G(\rho, \eta, \theta, \bar{\rho})f(\bar{\rho})\bar{\rho} d\bar{\rho} \quad (19)$$

Assume the distribution of a three-dimensional sink along the annulus  $(\bar{\rho}, \bar{\rho} + d\bar{\rho})$  of strength  $2f(\bar{\rho})\cos \theta$  (sketch (d)).



(d) Sketch of spherical tank showing coordinates of free surface. Top view.

The vertical velocities along  $\eta = 0$  vanish everywhere except on the strips of length  $d\bar{\rho}$  at  $\bar{\rho}$  and  $\rho$ . Only the mode for which  $\theta = 0$  is of interest since the excitation occurs in the X,Y-plane. Equation (19) becomes

$$f(\rho) = \lambda a \int_0^1 G(\rho, 0, 0, \bar{\rho})f(\bar{\rho})\bar{\rho} d\bar{\rho} \quad (20)$$

where the characteristic free surface is  $f(\rho)$  and the associated eigenvalues of  $\lambda a$  yield the natural frequencies. Let

$$W(\rho) = \sqrt{\rho} f(\rho) \quad (21)$$

then

$$W(\rho) = \lambda a \int_0^1 A(\rho, \bar{\rho}) W(\bar{\rho}) d\bar{\rho} \quad (22)$$

where

$$A(\rho, \bar{\rho}) = \sqrt{\rho \bar{\rho}} [G(\rho, 0, 0, \bar{\rho})]$$

The problem now is to determine  $A(\rho, \bar{\rho})$ .

In reference 10 the nearly full case is given as

$$A(\rho, \bar{\rho}) = \frac{2}{\pi} (\bar{\rho}/\rho)^{1/2} [K(\rho/\bar{\rho}) - E(\rho/\bar{\rho})] \quad (23)$$

and the half-full case as

$$A(\rho, \bar{\rho}) = \frac{2}{\pi} \left\{ (\bar{\rho}/\rho)^{1/2} [K(\rho/\bar{\rho}) - E(\rho/\bar{\rho})] + (\rho \bar{\rho})^{3/2} K(\rho \bar{\rho}) \right\} \quad (24)$$

for  $\rho < \bar{\rho} \neq 1$

Since equations (23) and (24) provide the essentials of the kernel function at two conditions, full and half full, it is necessary to introduce a factor that will define the kernel function for all depths. This requires a modification of the Budiansky equation by a multiplying factor empirically determined to be  $\gamma - 1$  where

$$\gamma = \frac{\pi}{\frac{\pi}{2} + \beta} \quad (25)$$

so that  $A(\rho, \bar{\rho})$  becomes

$$A(\rho, \bar{\rho}) = \frac{2}{\pi} (\bar{\rho}/\rho)^{1/2} [K(\rho/\bar{\rho}) - E(\rho/\bar{\rho})] + \frac{2}{\pi} (\gamma - 1) (\rho \bar{\rho})^{3/2} K(\rho \bar{\rho}) \quad (26)$$

for  $\rho < \bar{\rho} \neq 1$

$$A(\rho, \bar{\rho}) = \frac{1}{\pi} \left( \log \frac{8\rho}{|\epsilon|} - 2 \right) + (\gamma - 1) \left[ \frac{2\rho^3}{\pi} K(\rho^2) \right] \quad (27)$$

for  $\rho \approx \bar{\rho} \neq 1$

$$A(\rho, \bar{\rho}) = \frac{\gamma - 1}{\pi} \left( \log 8 + \log \frac{\Delta}{2} \right) \quad \text{for } \rho \approx \bar{\rho} = 1 \quad (28)$$

The terms  $K(\rho/\bar{\rho})$ ,  $E(\rho/\bar{\rho})$  are elliptic integrals of the first and second kind, respectively, (ref. 13) that can be approximated by

$$K(\rho/\bar{\rho}) = a_0 + a_1\xi + a_2\xi^2 + a_3\xi^3 + a_4\xi^4 \\ + \ln(1/\xi)(b_0 + b_1\xi + b_2\xi^2 + b_3\xi^3 + b_4\xi^4) \quad (29)$$

where

$$\begin{aligned} a_0 &= 1.3862944 & b_0 &= 0.5000000 \\ a_1 &= 0.0966634 & b_1 &= 0.1249859 \\ a_2 &= 0.0359009 & b_2 &= 0.0688025 \\ a_3 &= 0.0374256 & b_3 &= 0.0332835 \\ a_4 &= 0.0145120 & b_4 &= 0.0044179 \end{aligned}$$

$$E(\rho/\bar{\rho}) = 1 + a_{11}\xi + a_{21}\xi^2 + a_{31}\xi^3 + a_{41}\xi^4 \\ + \ln(1/\xi)(b_{11}\xi + b_{21}\xi^2 + b_{31}\xi^3 + b_{41}\xi^4) \quad (30)$$

where

$$\begin{aligned} a_{11} &= 0.4432514 & b_{11} &= 0.2499837 \\ a_{21} &= 0.0626060 & b_{21} &= 0.0920018 \\ a_{31} &= 0.0475738 & b_{31} &= 0.0406970 \\ a_{41} &= 0.0173651 & b_{41} &= 0.0052645 \end{aligned}$$

$$\text{for } 0 \leq \rho/\bar{\rho} < 1, \xi = 1 - (\rho/\bar{\rho})^2$$

The solution of equation (22) is essentially "N" simultaneous linear equations and can be handled easily as an eigenvalue problem. The solutions of the homogeneous integral equation

$$W(\rho) = \lambda a \int_0^1 A(\rho, \bar{\rho}) W(\bar{\rho}) d\bar{\rho} \quad (31)$$

will provide the characteristic free-surface shapes  $W(\rho)$ , the eigenvalues  $\lambda_n$ , and the function  $A(\rho, \bar{\rho})$ . The function  $A(\rho, \bar{\rho})$  is defined again as

$$A(\rho, \bar{\rho}) = \frac{2}{\pi} \left\{ \frac{1}{(\rho/\bar{\rho})^{1/2}} [K(\rho/\bar{\rho}) - E(\rho/\bar{\rho})] + (\gamma - 1)(\rho\bar{\rho})^{3/2} K(\rho\bar{\rho}) \right\} \quad (32)$$

for all tank depths  $\beta$ . Note that  $A(0, \bar{\rho}) = A(\rho, 0) = 0$  and that  $W(0) = 0$ .

The integral equation is now approximated by the matrix solution

$$AT\{W\} = \lambda_n\{W\} \quad (33)$$

where  $\{W\}$  is the column vector with elements  $W(j\Delta)$ ,  $\Delta = 1/N$ , and  $j = 1, 2, 3, \dots, N$ ,  $T$  is the integrating diagonal matrix, and

$$T_{i,i} = 1 \quad \text{for } i \neq N \quad (34)$$

$$T_{N,N} = 0.5 \quad (35)$$

The general elements of the symmetrical matrix  $A$  are defined by

$$A(i\Delta, j\Delta) = \frac{2}{\pi} \left\{ \frac{1}{\left(\frac{j\Delta}{i\Delta}\right)^{-1/2}} \left[ K\left(\frac{i\Delta}{j\Delta}\right) - E\left(\frac{i\Delta}{j\Delta}\right) \right] + (\gamma - 1) \left(\frac{i\Delta}{j\Delta}\right)^{3/2} K(i\Delta j\Delta) \right\} \quad \text{for } i \neq j \neq N \quad (36)$$

$$A(i\Delta, j\Delta) = \frac{1}{\pi} \left[ \log \frac{8}{\epsilon} + \log(i\Delta) - 2 + 2(\gamma - 1)(i\Delta)^3 K(i\Delta^2) \right] \quad \text{for } i = j \neq N \quad (37)$$

$$A(1, j\Delta) = \frac{\gamma - 1}{\pi} \left( \log 8 - \log \frac{\Delta}{2} \right) \quad \text{for } i \neq j = N \quad (38)$$

(See appendix A for derivation of eqs. (37) and (38).)

$$\bar{\lambda}_n = \frac{N}{a\lambda_n} \quad (39)$$

hence

$$a\lambda_n = \frac{N}{\bar{\lambda}_n} \quad (40)$$

The eigenvalues and eigenvectors of the matrix  $AT$  are found by matrix stripping (ref. 14). Let  $H_1 = A_1T$ ; then

$$H_2 = H_1 - \bar{\lambda}_1 \{W_1\} [W_1]T \quad (41)$$

where  $\{W_1\}$  is a column matrix and is the characteristic shape and  $[W_1]$  is a row matrix. This procedure is applied for  $n = 1, 2, 3$  modes. Figure 4 shows the wave forms  $W_n$  for various liquid depths. The eigenvalues and eigenvectors are shown in table I.

#### Comparison of Analytical and Experimental Frequencies

Figure 5 shows the theoretical calculations and experimental values of natural frequency parameters for the first three modes. The analytically determined critical frequencies are in excellent agreement when compared with the experimental results of this investigation and the results of reference 12. Use of the nondimensional frequency parameter renders the results independent of the density of the contained liquid for liquids having viscosities of approximately 1 centipoise. According to reference 12, the parameter made the results independent of tank size.

#### Analytical and Experimental Slosh Forces

Since the natural frequency parameters  $\lambda_n$  and the wave form  $W_n(\rho)$  have been determined, the slosh forces  $F_s$  can be calculated using the following equations (see ref. 10):

$$\ddot{\sigma}_n + \omega_n^2 \sigma_n = L_1 \ddot{u}(t) \quad (42)$$

$$(M_C + M_L) \ddot{u} + \pi \rho_L (aR)^3 \sum D_n \ddot{\sigma}_n = F_t \quad (43)$$

$$\ddot{u} M_C - F_t = F_s \quad (44)$$

where

$$L_1 = \frac{a \lambda_n D_n}{c_n} \quad (45)$$

$$c_n = \int_0^1 \rho [W_n(\rho)]^2 d\rho \quad (46)$$

$$D_n = \int_0^1 \rho^{3/2} W_n(\rho) d\rho \quad (47)$$

where  $\sigma_n$  is the slosh height at the wall associated with the  $n^{\text{th}}$  mode,  $\sum \sigma_n$  is the total height of slosh at the wall, the driving force is

$$\ddot{u}(t) = X_0 \alpha^2 \sin \alpha t$$

and

$$\omega_n = \sqrt{\lambda_n \frac{g}{R}}$$

(See figs. 6 and 7 for  $C_n$  and  $D_n$ , respectively.) Solution of these force equations is shown in appendix B.

The results of the analytical slosh-force calculations and experimental data are compared in figure 8 for liquid-depth ratios of 0.50 and 0.40. The slosh forces, which are presented as the dimensionless parameter  $F_s / \rho_L g d^3 (X_0/d)$ , are shown as a function of the oscillatory frequency parameter  $\alpha \sqrt{R/g}$ . At the natural modes, the slosh force is independent of the excitation amplitude  $X_0$ ; that is, the excitation amplitude influences only the time required for the waves to build and does not affect the maximum wave height or slosh forces. The value of  $X_0/d$  used was 0.0066.

The analytical and experimental slosh-force parameters, shown in figure 8, are in close agreement except at values of the oscillatory frequency parameter that correspond to the natural modes of the contained liquid. The maximum analytical and experimental values of the slosh-force parameter occur at a value of the oscillatory frequency parameter that corresponds to the first natural mode of the liquid (dashed lines in fig. 8). As the difference between the natural frequency and the driving frequency approaches zero, the analytical wave height  $\sigma_n$  and, in turn, the analytical slosh force  $F_s$  become very large (see sketch (e) in appendix B). Limiting the wave height to the distance between the undisturbed surface and the top of the tank in the analytical equations restricted the maximum force parameters at the first mode, but they were appreciably higher than the experimental data (>18 for the half-full tank). Experimentally, it was observed that (1) the slosh-force parameter was independent of the density of the contained liquid, (2) the maximum slosh forces near the first natural mode occurred at the maximum wave height obtainable without the waves breaking over or swirling in the tank, and (3) this maximum wave height was appreciably less than the distance between the undisturbed surface and the top of the tank. The swirl, or spinning, of the liquid in the tank occurred at frequencies very close to the natural modes, and the rotational frequency of the swirl was approximately equal to the frequency of the natural mode of the contained liquid.

Experimental values of slosh-force parameter are presented in figure 9 as a function of liquid-depth ratio for the first natural modes.

The slosh-force parameter increases with depth ratio to a maximum at the half-full condition ( $h/2R = 0.50$ ) and then decreases as the liquid depth increases. Thus, the maximum slosh forces will occur when a half-full tank is oscillated at the first natural mode frequency. The maximum experimental slosh forces were approximately equal to one-fourth the apparent weight of the contained liquid. It was also of interest to note that there was very little damping of the slosh forces with time (see fig. 3); that is, the forces continued for a relatively long period of time after the tank had been quick-stopped.

The different slosh-force-parameter levels appearing at any given value of the oscillatory frequency parameter (figs. 8 and 9) are due to experimental technique. The tank was oscillated, and the waves were allowed to build to a maximum height (determined visually) without breaking and rolling over in the tank; then the tank was quick-stopped. At frequencies near the first mode, the waves would build very rapidly and tend to break and swirl in the tank. Maximum slosh forces occurred just before the waves broke. The scatter of the data is attributed to the difficulty in quick-stopping the tank at the proper time.

#### CONCLUDING REMARKS

The analytical equations of reference 10, relating to the modes and frequencies of specific liquid depths in the spherical tank, were augmented and modified to achieve equations applicable to arbitrary liquid depths. These modified equations and the force equations of references 10 and 11 were applied in predicting the natural frequencies and slosh forces. Experimentally determined natural frequencies and slosh forces were compared with the analytically predicted values.

In consideration of the nearly empty to the nearly full spherical tank, the experimental results served to verify the analytical methods for predicting: (1) the natural frequencies of the contained liquid, and (2) the slosh forces for varying disturbing frequencies except at disturbing frequencies very near the fundamental frequency. The maximum experimental slosh forces, which are approximately equal to one-fourth the apparent weight of the liquid, occurred at the first fundamental frequency of the liquid for the half-full tank. Use of nondimensional frequency and force parameters made the results independent of the contained liquid density and tank size.

Lewis Research Center

National Aeronautics and Space Administration  
Cleveland, Ohio, March 13, 1962

## APPENDIX A

SPECIAL CONSIDERATIONS OF LOGARITHMIC SINGULARITIES  
OF THE KERNEL FUNCTION  $A(\rho, \bar{\rho})$ 

Consideration is given to the special condition of the function  $A(\rho, \bar{\rho})$  as  $\rho \rightarrow \bar{\rho} \neq 1$ , where

$$A(\rho, \bar{\rho}) = \frac{2}{\pi} \frac{1}{(\rho/\bar{\rho})^{1/2}} \left[ K(\rho/\bar{\rho}) - E(\rho/\bar{\rho}) \right] + \frac{2}{\pi} (\gamma - 1) (\rho\bar{\rho})^{3/2} K(\rho\bar{\rho}) \quad (A1)$$

Let

$$\Gamma = \rho/\bar{\rho} \quad (A2)$$

Equation (A1) then becomes

$$A(\rho, \bar{\rho}) = \frac{2}{\pi} \frac{1}{\Gamma^{1/2}} \left[ K(\Gamma) - E(\Gamma) \right] + \frac{2}{\pi} (\gamma - 1) \rho^3 K(\rho^2) \quad (A3)$$

where

$$K(\Gamma) = \int_0^{\pi/2} \frac{d\phi}{\sqrt{1 - \Gamma^2 \sin^2 \phi}} \quad (A4)$$

and

$$E(\Gamma) = \int_0^{\pi/2} \sqrt{1 - \Gamma^2 \sin^2 \phi} \, d\phi \quad (A5)$$

These are complete elliptic functions of the first and second kind, respectively. It is noted that as  $\Gamma \rightarrow 1$  the  $K(\Gamma)$  function approaches infinity, while  $E(\Gamma) \rightarrow 1$ ; hence, it becomes necessary to study the manner in which  $K(\Gamma)$  approaches infinity. Let

$$Z = \Gamma \sin \phi \quad (A6)$$

In order to evaluate the integral, the integrand is expanded by the binomial theorem

$$\frac{1}{\sqrt{1 - Z^2}} = 1 + \frac{1}{2} Z^2 + \frac{1}{2} \times \frac{3}{4} Z^4 + \dots \quad (A7)$$

and then integrated term by term. For  $\Gamma^2 < 1$  this series will converge uniformly for all values of  $\phi$ . Substituting for  $Z$  yields

$$\begin{aligned}
 K(\Gamma) &= \int_0^{1/2} \frac{d\phi}{\sqrt{1-Z^2}} = \int_0^{\pi/2} d\phi + \frac{1}{2} \Gamma^2 \int_0^{\pi/2} \sin^2\phi \, d\phi \\
 &+ \frac{1}{2} \times \frac{3}{4} \Gamma^4 \int_0^{\pi/2} \sin^4\phi \, d\phi + \dots \left( \frac{1}{2} \times \frac{3}{4} \dots \frac{2n-1}{2n} \right) \Gamma^{2n} \int_0^{\pi/2} \sin^{2n}\phi \, d\phi
 \end{aligned}
 \tag{A8}$$

which on integration yields

$$K(\Gamma) = \frac{\pi}{2} \left[ 1 + \left(\frac{1}{2}\right)^2 \Gamma^2 + \left(\frac{1}{2} \times \frac{3}{4}\right)^2 \Gamma^4 \dots \left(\frac{1}{2} \times \frac{3}{4} \dots \frac{2n-1}{2n}\right)^2 \Gamma^{2n} + \dots \right]
 \tag{A9}$$

As  $\Gamma^2$  becomes approximately equal to 1, equation (A9), in powers of  $\Gamma^2 \approx 1$ , yields

$$\begin{aligned}
 K(\Gamma) &= \frac{\pi}{2} \left[ \ln \frac{4}{\sqrt{1-\Gamma^2}} + \left( \ln \frac{4}{\sqrt{1-\Gamma^2}} - 1 \right) \left(\frac{1}{2}\right)^2 \Gamma^2 \right. \\
 &\quad \left. + \left(\frac{1}{2} \times \frac{3}{4}\right)^2 \left( \ln \frac{4}{\sqrt{1-\Gamma^2}} - \frac{7}{6} \right) \Gamma^4 \dots \right]
 \end{aligned}
 \tag{A10}$$

If  $\Gamma$  is assumed near unity, the convergence of the preceding series (eq. (A10)) is such that the first several terms are all that would be necessary to arrive at  $K(\Gamma)$  accurate to four decimal places:

$$K(\Gamma) \approx \frac{1}{2} \ln \frac{8}{1-\Gamma}
 \tag{A11}$$

Substituting for  $\Gamma$  yields

$$K(\Gamma) = \frac{1}{2} \ln \frac{8\rho}{|\bar{\rho} - \rho|}
 \tag{A12}$$

hence,

$$K(\Gamma) = \log 8 + \log \rho - \log |\bar{\rho} - \rho|
 \tag{A13}$$

From equation (A5) it is obvious that as  $\Gamma \rightarrow 1$

$$E(1) = 1
 \tag{A14}$$

Substitution of equations (A13) and (A14) into equation (A3), with  $\bar{\rho} \approx \rho \neq 1$ , yields

$$A(\rho, \bar{\rho}) = \frac{1}{\pi} \log \frac{8\rho}{|\bar{\rho} - \rho|} - \frac{2}{\pi} + \frac{2}{\pi} (\gamma - 1) \rho^3 K(\rho^2) \quad (\text{A15})$$

Note that at  $\bar{\rho} = \rho \neq 1$  the function is undefined; furthermore, a choice of  $\bar{\rho} - \rho = \epsilon$  yields

$$A(\rho, \bar{\rho}) = \frac{1}{\pi} \log \frac{8\rho}{|\epsilon|} - \frac{2}{\pi} + \frac{2}{\pi} (\gamma - 1) \rho^3 K(\rho^2) \quad (\text{A16})$$

$$A(1, \bar{\rho}) = \frac{\gamma - 1}{\pi} \left( \log 8 - \log \frac{\Delta}{2} \right)$$

$$\text{for } \bar{\rho} \approx \rho = 1 \quad (\text{A17})$$

## APPENDIX B

## DERIVATION OF FORCE EQUATION

Consider the system to be governed by the differential equation

$$\left. \begin{aligned} \ddot{\sigma}_n + \omega_n^2 \sigma_n &= -L_1 X_0 \alpha^2 \sin \alpha t \\ \ddot{\sigma}_n &= -\omega_n^2 \sigma_n - L_1 X_0 \alpha^2 \sin \alpha t \end{aligned} \right\} \quad (B1)$$

The general solution is

$$\sigma_n = L_2 X_0 \alpha^2 \sin \alpha t + L_3 \sin \omega_n t + L_4 \cos \omega_n t \quad (B2)$$

$$\dot{\sigma}_n = L_2 X_0 \alpha^3 \cos \alpha t + L_3 \omega_n \cos \omega_n t - L_4 \omega_n \sin \omega_n t \quad (B3)$$

$$\left. \begin{aligned} t_0 &= 0 \\ \sigma_n(0) &= 0 \\ L_4 &= 0 \end{aligned} \right\} \quad (B4)$$

$$\dot{\sigma}_n(0) = 0 = L_2 X_0 \alpha^3 + L_3 \omega_n \quad (B5)$$

$$L_3 = -L_2 X_0 \frac{\alpha^3}{\omega_n} \quad (B6)$$

Substitution of equation (B6) into equation (B2) yields

$$\sigma_n = L_2 X_0 \alpha^2 \sin \alpha t - L_2 X_0 \frac{\alpha^3}{\omega_n} \sin \omega_n t \quad (B7)$$

$$\ddot{\sigma}_n = -L_2 X_0 \alpha^4 \sin \alpha t + L_2 X_0 \alpha^3 \omega_n \sin \omega_n t \quad (B8)$$

Solution for  $L_2$  using equations (B1) and (B8) yields

$$\begin{aligned} -L_2 X_0 \alpha^4 \sin \alpha t + L_2 X_0 \alpha^3 \omega_n \sin \omega_n t &= -\omega_n^2 L_2 X_0 \alpha^2 \sin \alpha t \\ &+ \omega_n L_2 X_0 \alpha^3 \sin \omega_n t - L_1 X_0 \alpha^2 \sin \alpha t \end{aligned} \quad (B9)$$

Finally,

$$L_2 = -\frac{L_1}{\omega_n^2 - \alpha^2} \quad (B10)$$

Let  $L_1 = \alpha \lambda_n (D_n/C_n)$ ; then equation (B7) becomes

$$\left. \begin{aligned} \sigma_n &= -\frac{L_1}{\omega_n^2 - \alpha^2} X_0 \alpha^2 \sin \alpha t + \frac{L_1}{\omega_n^2 - \alpha^2} X_0 \frac{\alpha^3}{\omega_n} \sin \omega_n t \\ \sigma_n &= \frac{L_1}{\omega_n^2 - \alpha^2} X_0 \alpha^2 \left( \frac{\alpha}{\omega_n} \sin \omega_n t - \sin \alpha t \right) \end{aligned} \right\} \quad (\text{B11})$$

for  $\alpha \neq \omega_n$

Let  $\alpha \rightarrow \omega_n$ ; then

$$\lim_{\alpha \rightarrow \omega_n} \sigma_n = \left[ \frac{\frac{d}{d\alpha} (\alpha^3 \sin \omega_n t - \alpha^3 \sin \alpha t)}{\frac{d}{d\alpha} (\omega_n^2 - \alpha^2)} \right] L_1 X_0 \quad (\text{B12})$$

$$\sigma_n = -\left[ \frac{3}{2} \frac{\alpha}{\omega_n} \sin \omega_n t + \sin \alpha t + \frac{\alpha}{2} t \cos \alpha t \right] L_1 X_0 \quad (\text{B13})$$

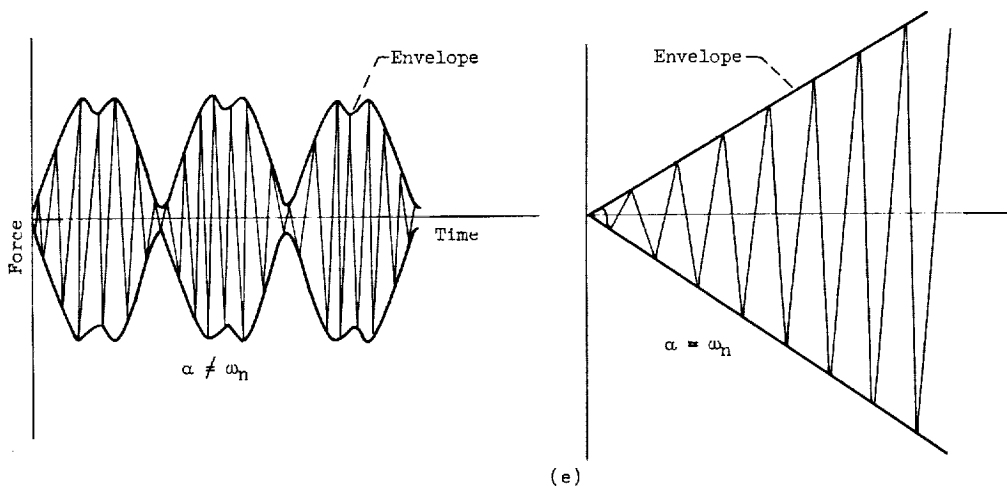
Since  $\alpha = \omega_n$ ,

$$\sigma_n = -\left( \frac{\sin \omega_n t + \omega_n t \cos \omega_n t}{2} \right) L_1 X_0 \quad (\text{B14})$$

or

$$\lim_{\alpha \rightarrow \omega_n} \sigma_n = \frac{L_1 X_0}{2} (\omega_n t \cos \omega_n t - \sin \omega_n t) \quad (\text{B15})$$

The following sketches show the theoretical slosh forces and the envelope of the slosh forces for the two conditions  $\alpha \neq \omega_n$  and  $\alpha = \omega_n$ .



## REFERENCES

1. Abramson, H. Norman, and Ransleben, Guido E., Jr.: Simulation of Fuel Sloshing Characteristics in Missile Tanks by Use of Small Models. Tech. Rep. 7, Southwest Res. Inst., April 25, 1960.
2. Abramson, H. Norman, and Ransleben, Guido E., Jr.: A Note on Wall Pressure Distributions During Sloshing in Rigid Tanks. Tech. Rep. 5, Southwest Res. Inst., June 15, 1959.
3. Abramson, H. Norman, and Ransleben, Guido E., Jr.: A Note on the Effectiveness of Two Types of SLOSH Suppression Devices. Tech. Rep. 6, Southwest Res. Inst., June 15, 1959.
4. Bauer, Helmut F.: Fluid Oscillations in a Circular Cylindrical Tank. Rep. DA-TR-1-58, Army Ballistic Missile Agency, Apr. 18, 1958.
5. Bauer, Helmut F.: Fluid Oscillation in a Cylindrical Tank with Damping. Rep. DA-TR-4-58, Army Ballistic Missile Agency, Apr. 23, 1958.
6. Bauer, Helmut F.: Propellant Sloshing. Rep. DA-TR-18-58, Army Ballistic Missile Agency, Nov. 5, 1958.
7. O'Neill, J. P.: An Experimental Investigation of Sloshing. STL-TR-59-0000-09960, Space Tech. Labs., Inc., March 4, 1960.
8. Leonard, H. Wayne, and Walton, William C., Jr.: An Investigation of the Natural Frequencies and Mode Shapes of Liquids in Oblate Spheroidal Tanks. NASA TN D-904, 1961.
9. McCarty, John Locke, Leonard, H. Wayne, and Walton, William C., Jr.: Experimental Investigation of the Natural Frequencies of Liquids in Toroidal Tanks. NASA TN D-531, 1960.
10. Budiansky, Bernard: Sloshing of Liquids in Circular Canals and Spherical Tanks. Jour. Aero/Space Sci., vol. 27, no. 3, Mar. 1960, pp. 161-173.
11. Lamb, Horace.: Hydrodynamics. Sixth ed., Dover Pub., 1945.
12. McCarty, John Locke, and Stephens, David G.: Investigation of the Natural Frequencies of Fluids in Spherical and Cylindrical Tanks. NASA TN D-252, 1960.
13. Hastings, C.: Approximations for Digital Computers. Princeton Univ. Press, 1955, p. 172.
14. Faddeeva, V. N.: Computational Methods of Linear Algebra. Dover Pub., 1959, p. 211.

TABLE I. - EIGENVALUES AND EIGENVECTORS FOR SPHERICAL TANK

| Liquid-depth ratio,<br>$h/2R$ | Tank-depth parameter,<br>$a$ | Eigenvalue   |              |              | Natural frequency parameter |                    |                    |
|-------------------------------|------------------------------|--------------|--------------|--------------|-----------------------------|--------------------|--------------------|
|                               |                              | $a\lambda_1$ | $a\lambda_2$ | $a\lambda_3$ | $\sqrt{\lambda_1}$          | $\sqrt{\lambda_2}$ | $\sqrt{\lambda_3}$ |
| 0.1                           | 0.6                          | 0.6708       | 4.6230       | 8.1145       | 1.0573                      | 2.7758             | 3.6775             |
| .2                            | .8                           | .9571        | 4.9787       | 8.4136       | 1.0938                      | 2.4947             | 3.2430             |
| .3                            | .9165                        | 1.1850       | 5.1612       | 8.5773       | 1.1370                      | 2.3731             | 3.0592             |
| .4                            | .9798                        | 1.3858       | 5.2883       | 8.6923       | 1.1893                      | 2.3232             | 2.9785             |
| .5                            | 1.0000                       | 1.5728       | 5.3910       | 8.7847       | 1.2540                      | 2.3218             | 2.9639             |
| .6                            | .9798                        | 1.7532       | 5.4827       | 8.8658       | 1.3376                      | 3.3655             | 3.0080             |
| .7                            | .9165                        | 1.9345       | 5.5712       | 8.9425       | 1.4528                      | 2.4655             | 3.1236             |
| .8                            | .8                           | 2.1254       | 5.6638       | 9.0209       | 1.6300                      | 2.6608             | 3.3580             |
| .9                            | .6                           | 2.3451       | 5.7732       | 9.1114       | 1.9770                      | 3.1019             | 3.8969             |

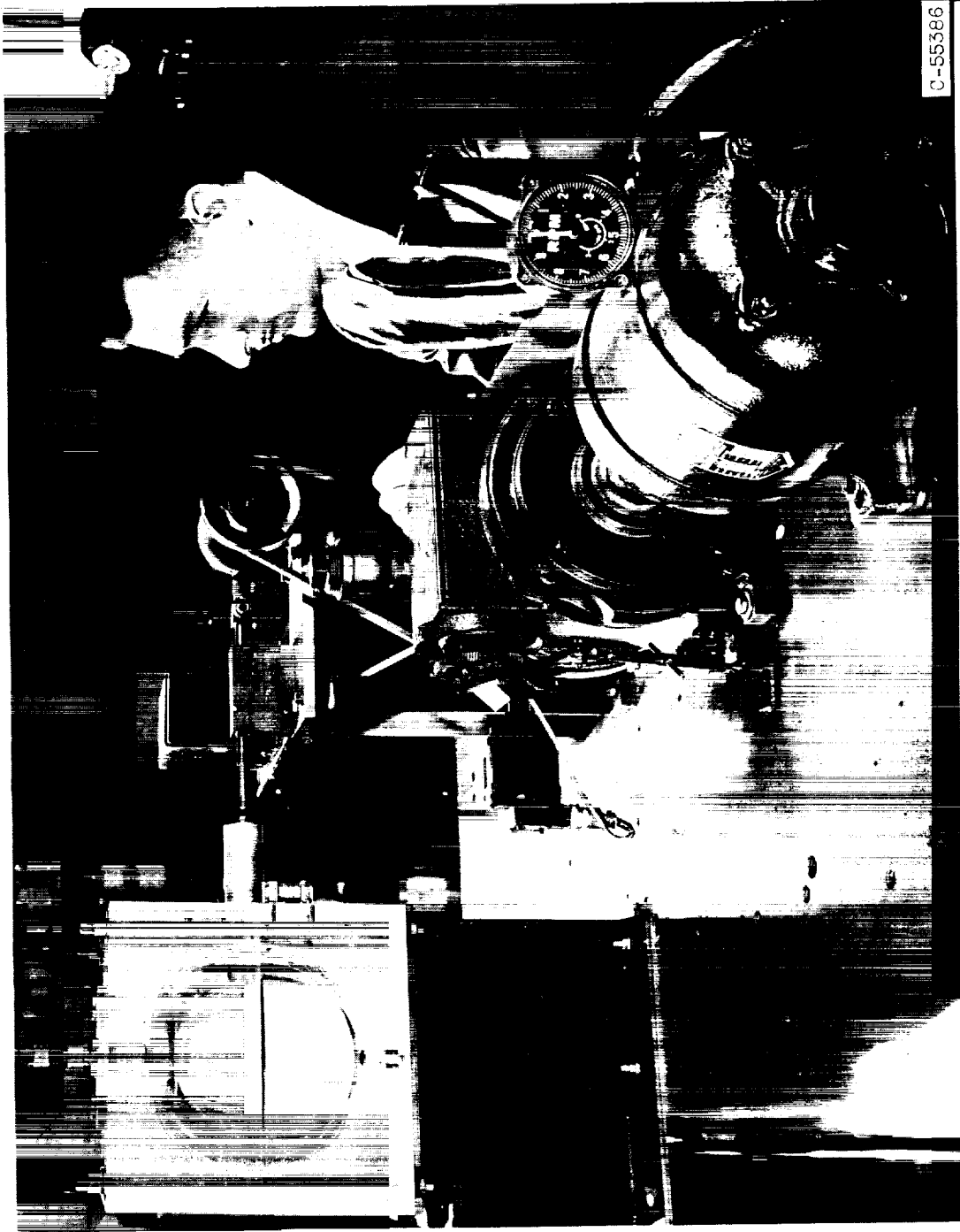


Figure 1. - Experimental test facility.



Figure 2. - Strain-gage mount.

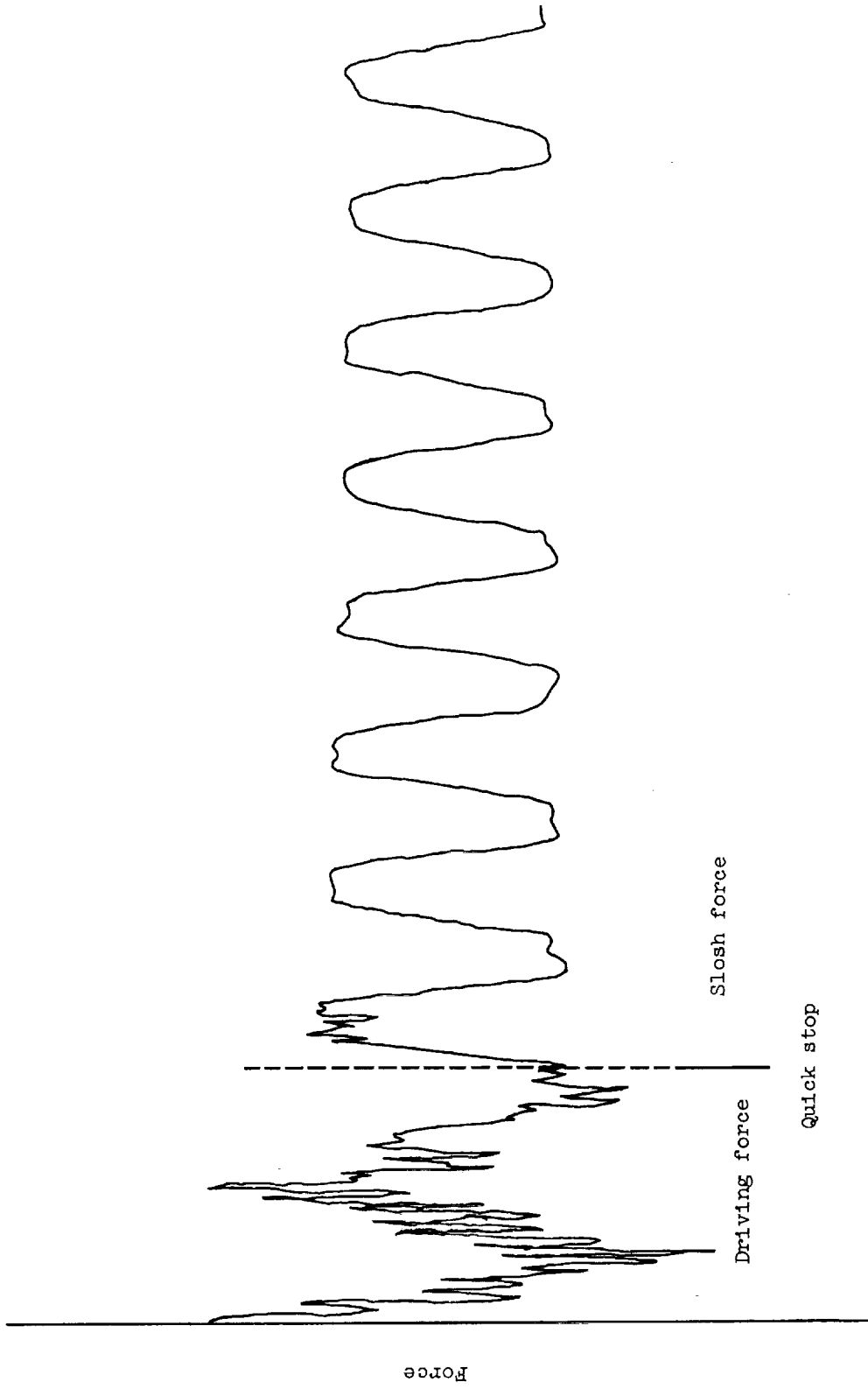
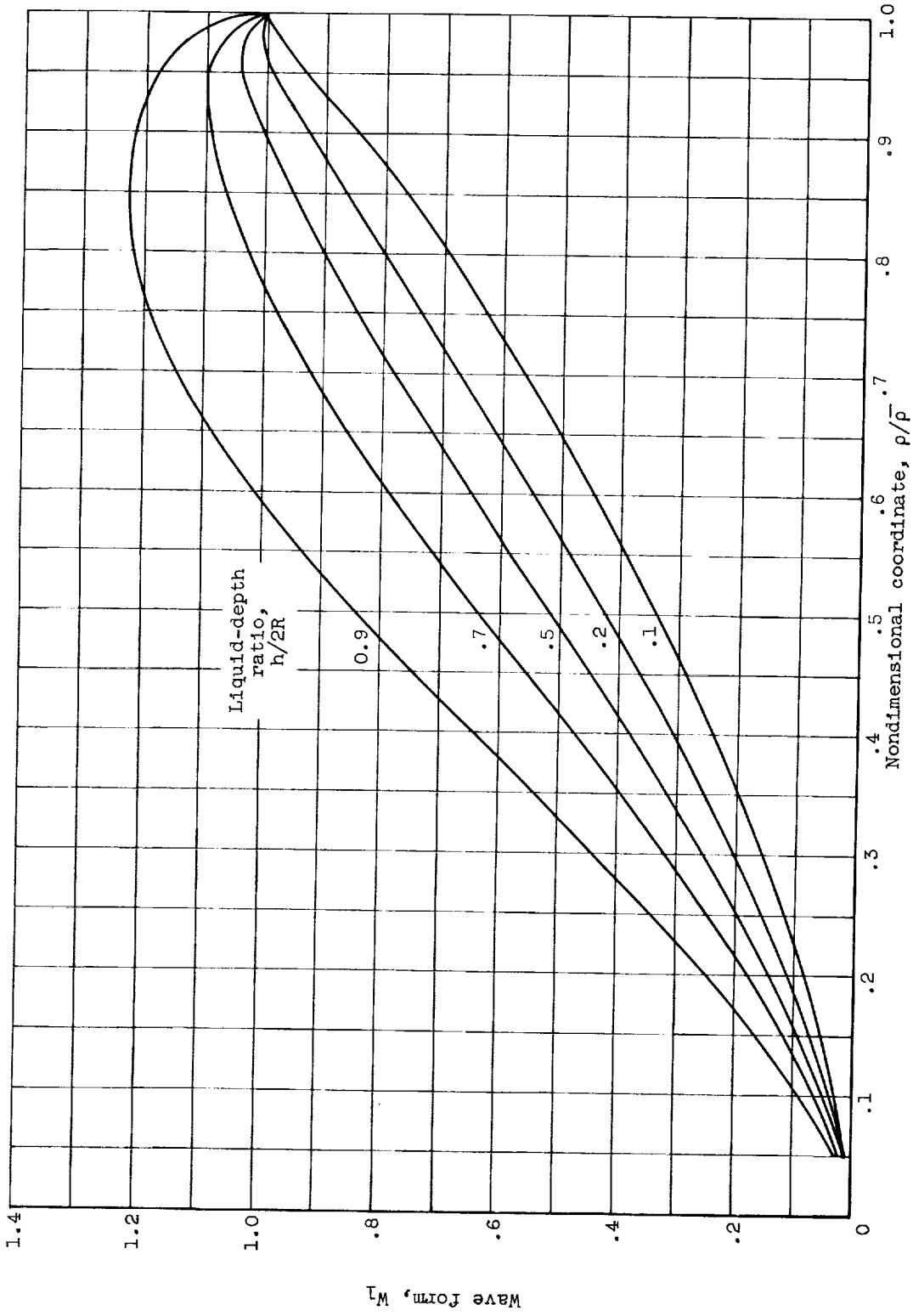
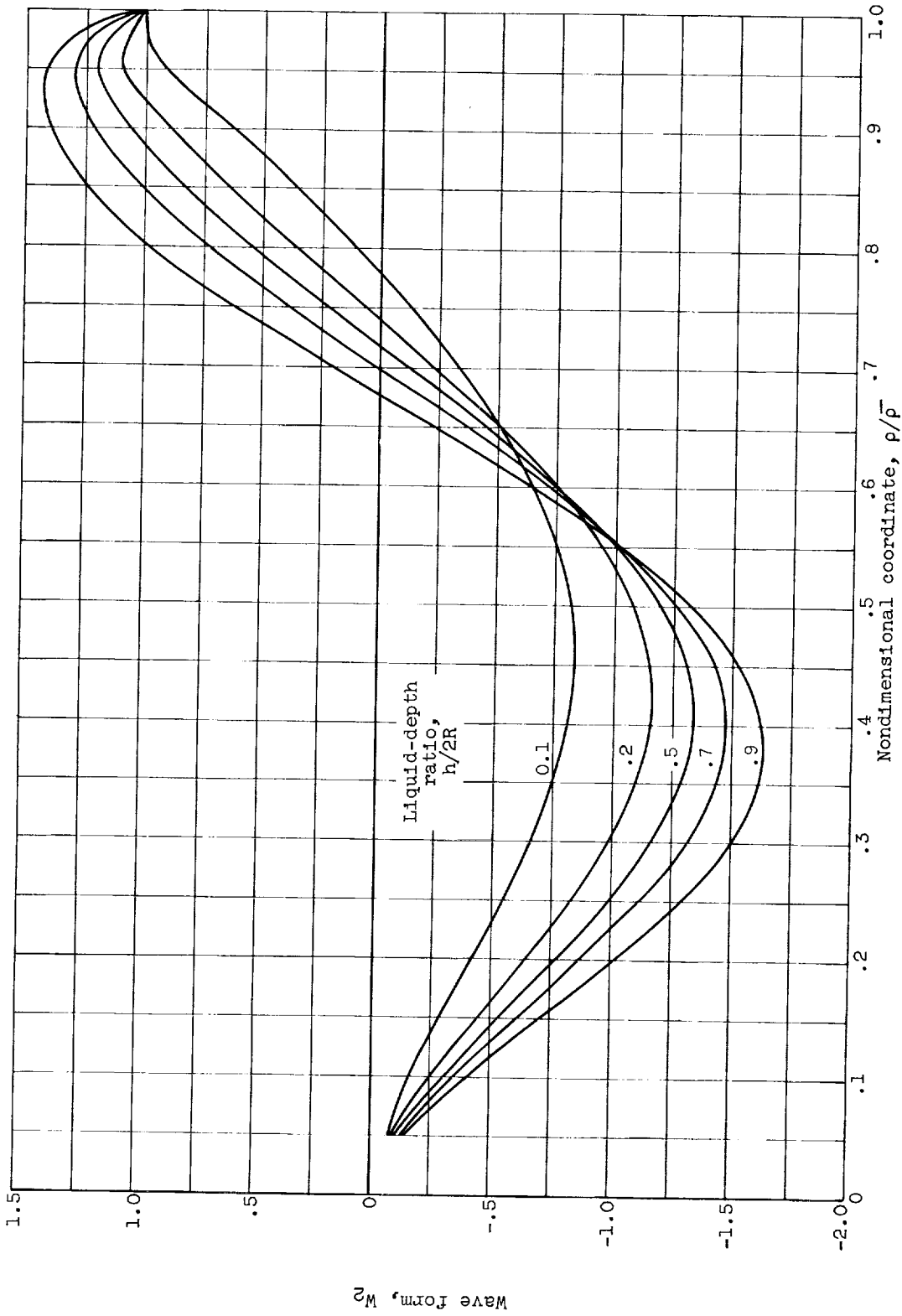


Figure 3. - Typical slosh-force trace. First mode; liquid-depth ratio,  $h/2R$ , 0.40.



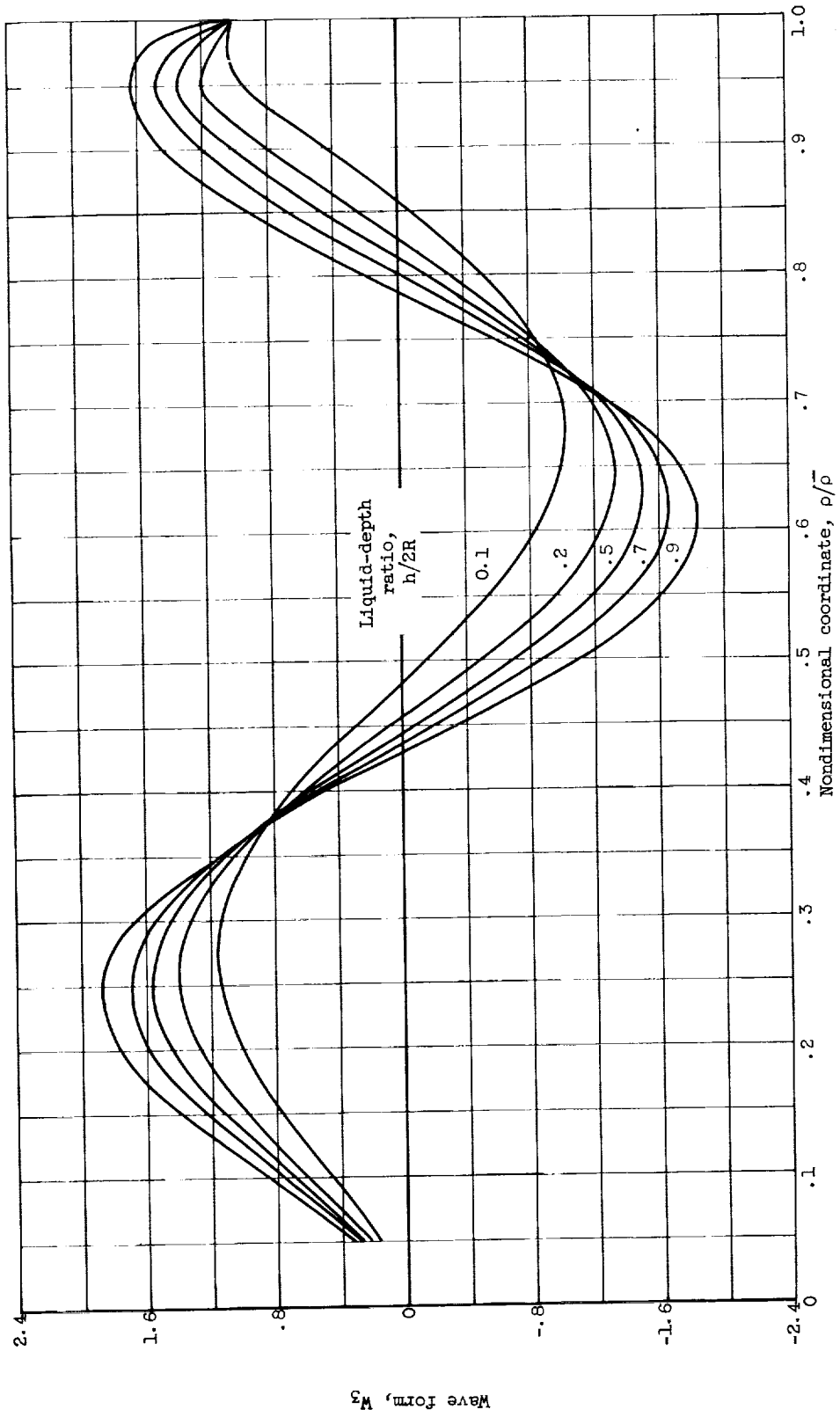
(a) First mode.

Figure 4. - Wave forms for various liquid-depth ratios.



(b) Second mode.

Figure 4. - Continued. Wave forms for various liquid-depth ratios.



(c) Third mode.

Figure 4. - Concluded. Wave forms for various liquid-depth ratios.

E-1435

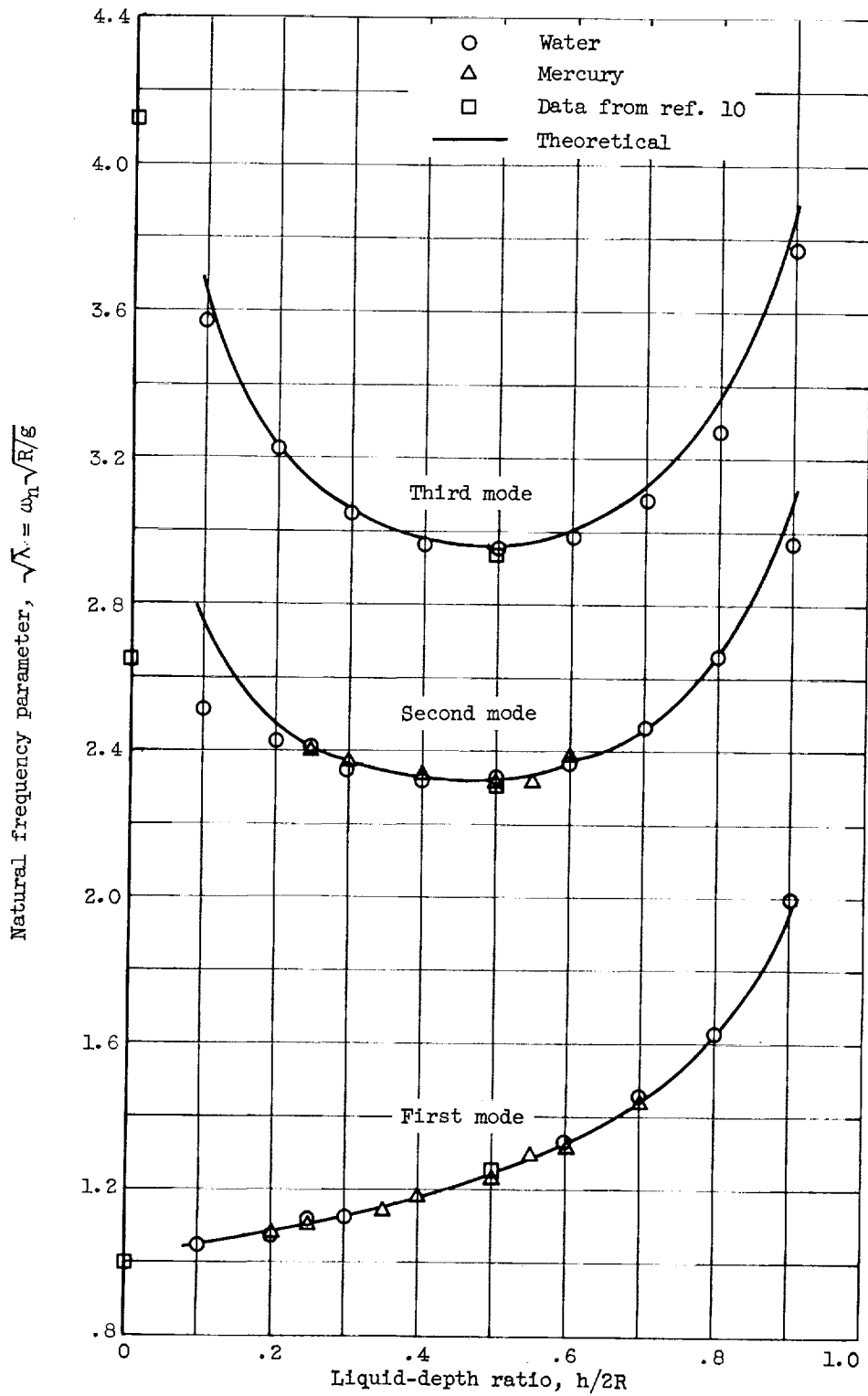


Figure 5. - Theoretical and experimental values of natural frequency parameters for first three modes.

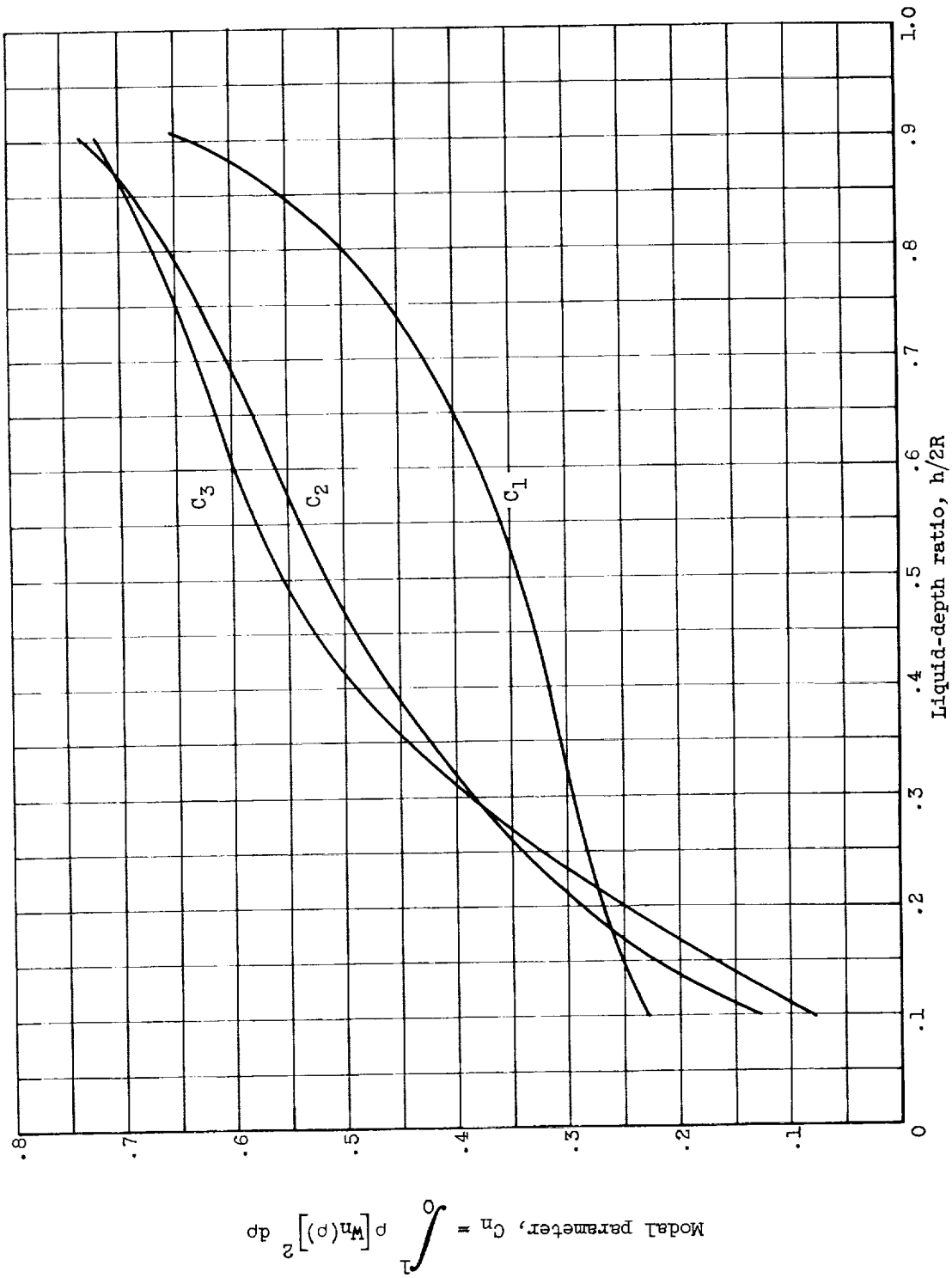


Figure 6. - Modal parameter  $C_n$  as function of liquid-depth ratio.

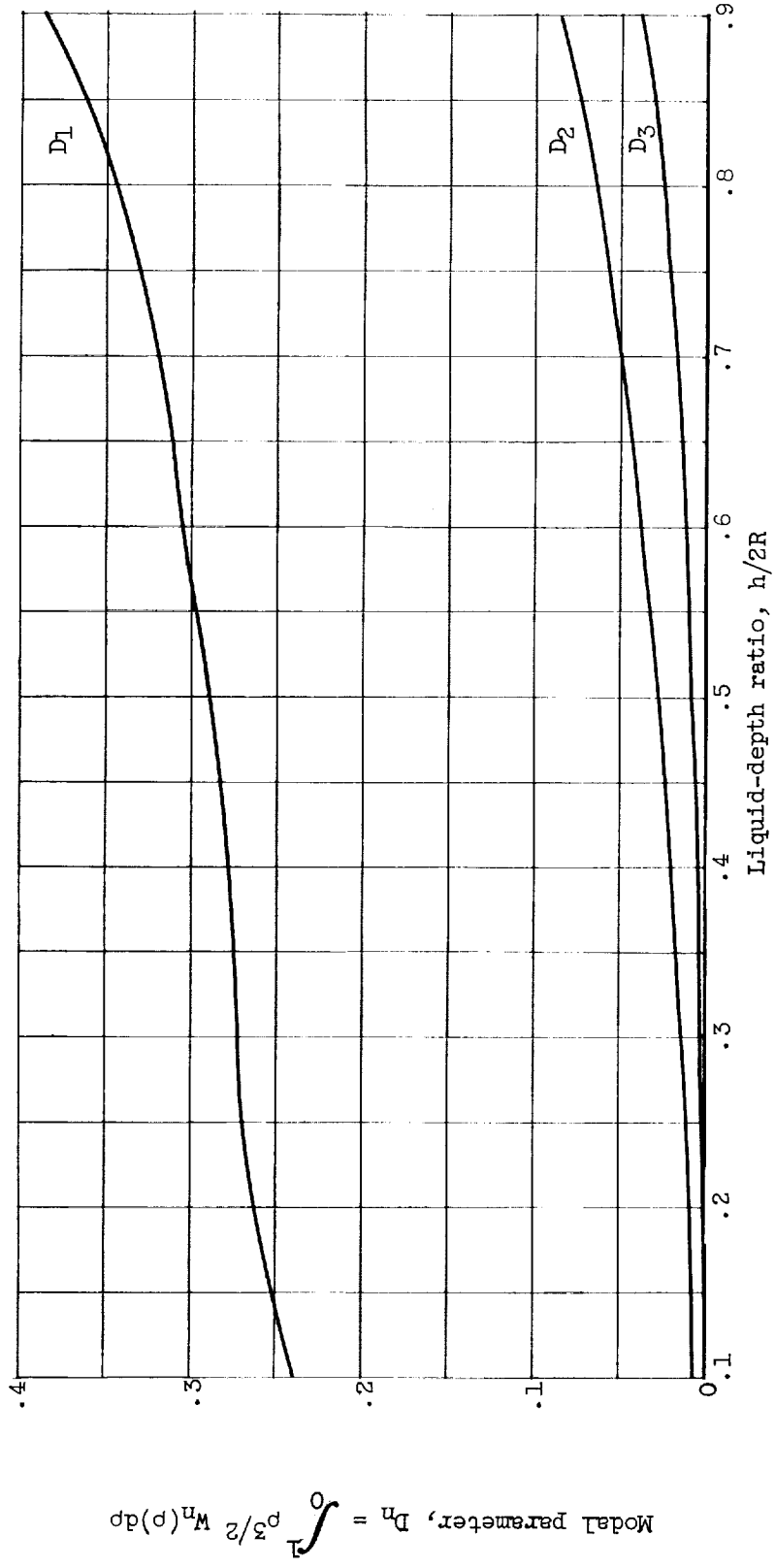
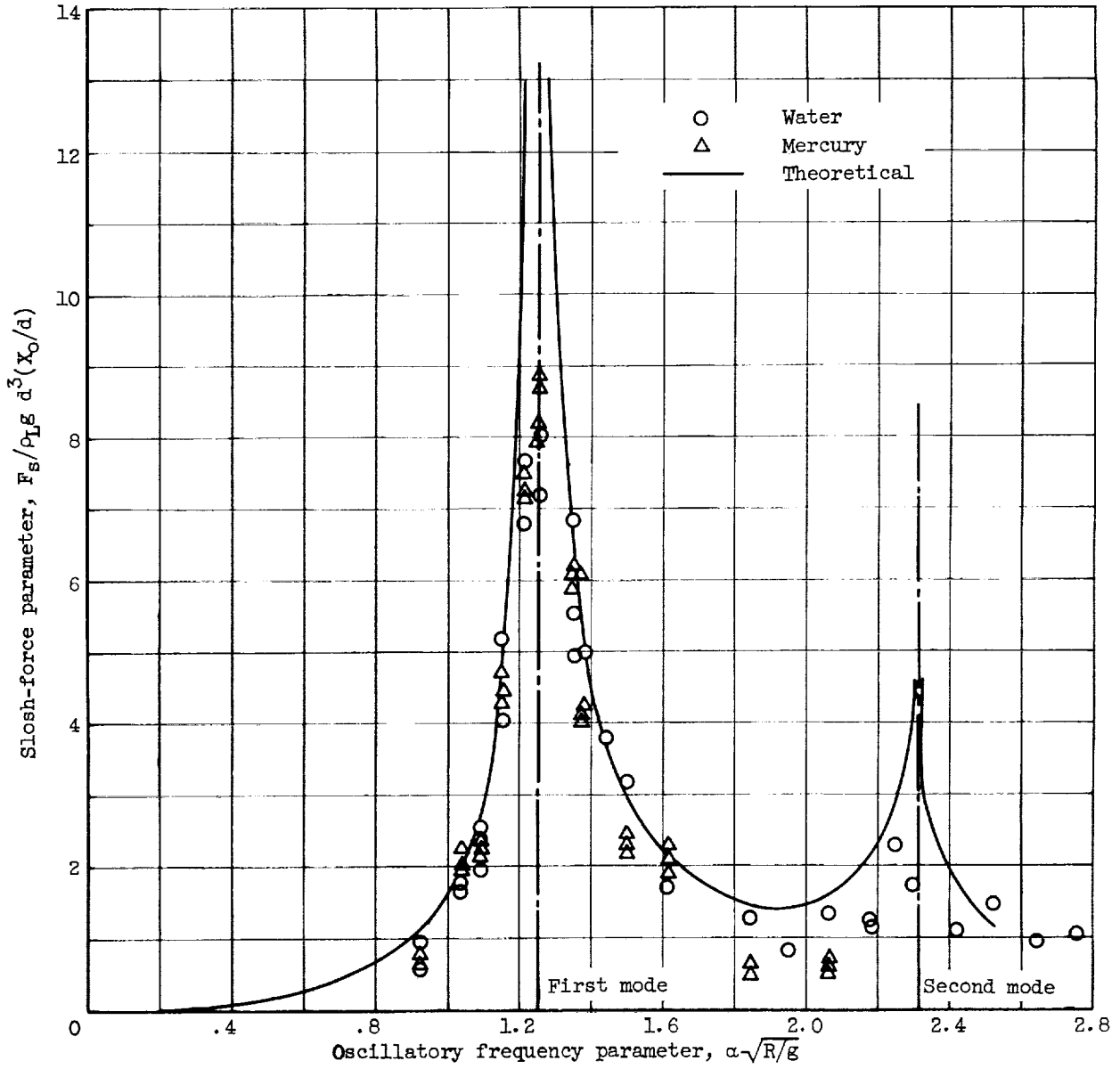


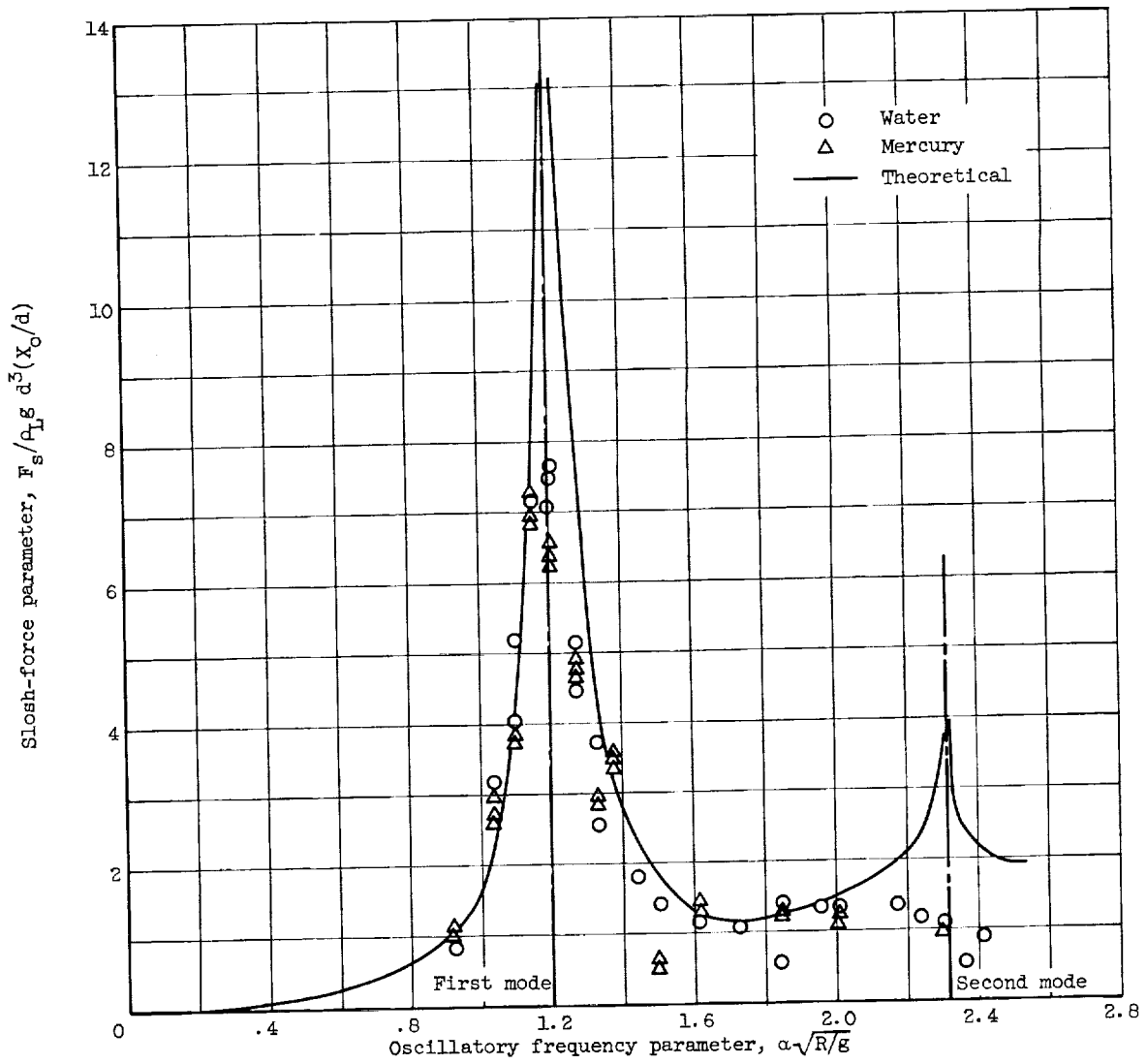
Figure 7. - Modal parameter  $D_n$  as function of liquid-depth ratio.



(a) Liquid-depth ratio,  $h/2R$ , 0.50.

Figure 8. - Slosh-force parameter as function of oscillatory frequency parameter.

W-1455



(b) Liquid-depth ratio,  $h/2R$ , 0.40.

Figure 8. - Concluded. Slosh-force parameter as function of oscillatory frequency parameter.

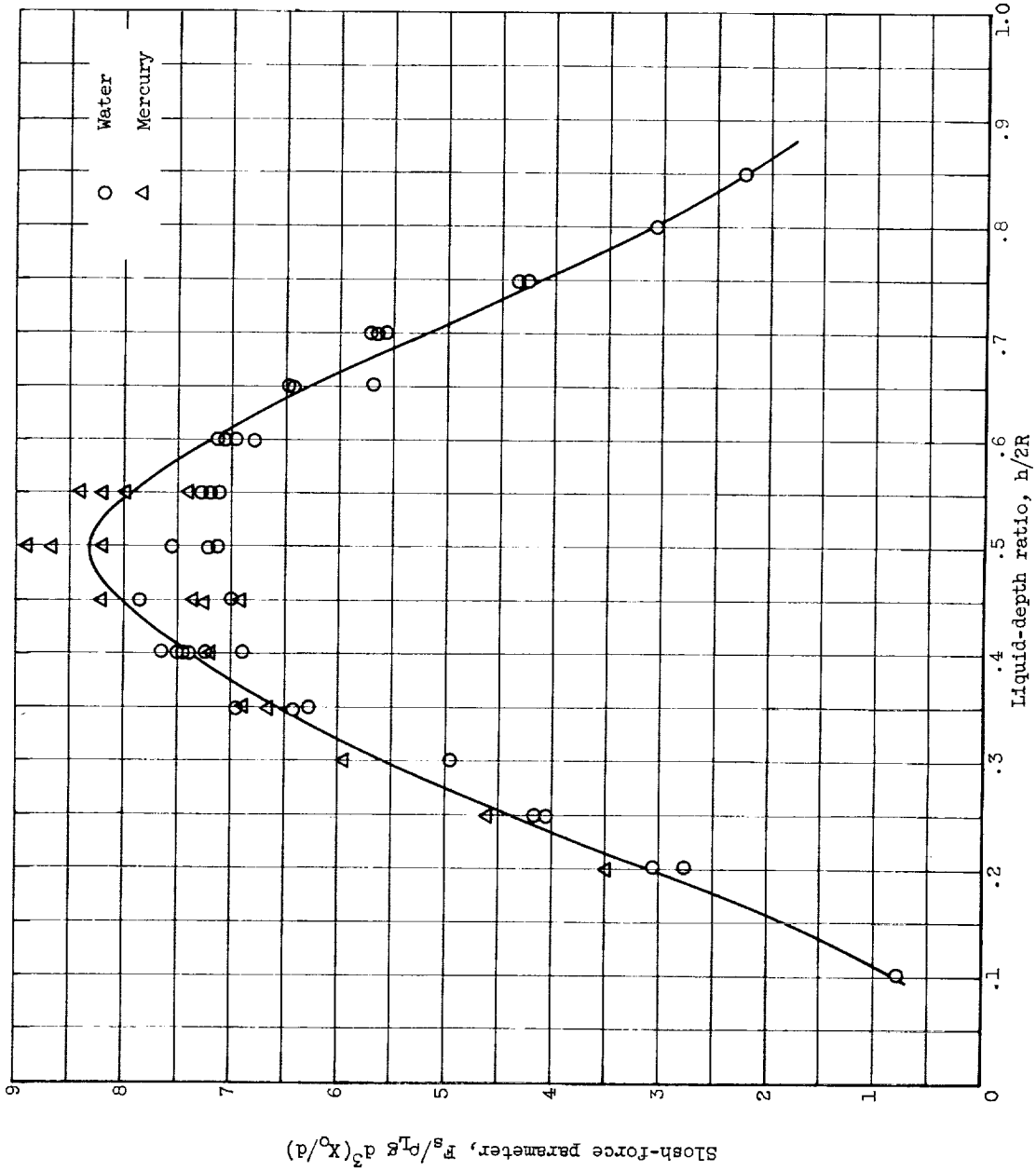


Figure 9. - Slosh-force parameter as function of liquid-depth ratio for first natural modes.